

## Bose-Einstein correlation of particles produced by expanding sources

Y. Hama and Sandra S. Padula

*Instituto de Física, Universidade de São Paulo, São Paulo, Brazil*

(Received 3 December 1987)

Bose-Einstein correlation is discussed for particles produced by rapidly expanding sources, when kinematical effects hinder a direct relation between the observed correlations and the source dimensions. Some of these effects are illustrated by considering Landau's hydrodynamical model wherein each space-time point of the fluid with temperature  $T = T_c \simeq m_\pi$  is taken as an independent and chaotic emitting center with a Planck spectral distribution. In particular, this model reproduces surprisingly well the observed  $\pi$ - $\pi$  and  $K$ - $K$  correlations at the CERN ISR.

### I. INTRODUCTION

The correlation between identical particles produced in a reaction is closely related to the space-time structure of the emitting source of these particles. This is the base of the Hanbury-Brown and Twiss method,<sup>1</sup> used in radio astronomy to measure stellar dimensions, and also of the Goldhaber-Goldhaber-Lee-Pais (GGLP) effect<sup>2</sup> in nuclear physics. Several authors have studied this phenomenon,<sup>3-7</sup> but so far concrete applications have mostly been restricted to static sources, the ones with factorized time and space dependences or field-theoretical model with a classical source.<sup>3</sup> While these models clarify several qualitative features of the phenomenon or even are convenient approximations in some cases, it is questionable to straightforwardly apply their results and try to extract from the data quantitative information on more dynamical processes such as hadronic interactions. In these reactions, the particle sources typically move at relativistic velocities with respect to each other and important kinematical effects appear preventing us from establishing a well-known simple relation between the observed correlations and the source dimensions.

In a previous paper,<sup>8</sup> we gave a preliminary account of our study of the identical-particle correlation, by using Landau's hydrodynamic model as a prototype of such a rapidly expanding particle source. Related discussions have recently been made by some other authors by using either the string-fragmentation model<sup>9</sup> or a current-ensemble method in the inside-outside cascade picture.<sup>10</sup> In the present paper, we shall give a more intuitive presentation of several of the effects caused by the emission-source motions, by considering a simple two-point-source model (Sec. II) and then illustrating them by a more realistic hydrodynamical model (Sec. III). For comparison with data, which will be achieved in Sec. IV, it is crucial to consider the emission of quanta throughout the whole phase transition, during which the energy density decreases from the initial value  $\epsilon_{pi}(T_c)$ , calculated for the plasma phase, down to  $\epsilon_h(T_c)$ , computed for the hadron gas. We will draw conclusions and propose some experimental works in Sec. V.

### II. TWO-POINT-SOURCE MODEL

By considering the simplest model of two pointlike sources we illustrate some interesting features concerning the sizes revealed by the correlation function when the sources are in movement with respect to each other: (a) the effective longitudinal distance decreases with increasing transversal momentum ( $p_T$ ); (b) the effective transversal depth depends on the emission time difference; (c) the correlation-function intercept can be smaller than 2 for finite values of momentum difference.

Let us consider two pointlike sources with space-time localizations given by  $x'^\mu = (t', \mathbf{r}')$  and  $x''^\mu = (t'', \mathbf{r}'')$  which independently emit quanta (pions) at random during a finite time interval  $\delta t$ . The correlation function can be written as

$$C(p_1, p_2) = \frac{W(p_1, p_2)}{W(p_1)W(p_2)} = 1 + \langle \cos(\Delta p^\mu \Delta x_\mu) \rangle, \quad (1)$$

where  $\Delta p^\mu = (E_2 - E_1, \mathbf{p}_2 - \mathbf{p}_1)$  and  $\Delta x^\mu = (t'' - t', \mathbf{r}'' - \mathbf{r}')$ ;  $W(p_1, p_2)$  is the probability for detecting two quanta in coincidence and  $W(p_i)$  is the single-particle probability. For the sake of simplicity the average symbol ( $\langle \rangle$ ) in (1) was introduced to represent integration over  $t'$  and  $t''$  with appropriate source-velocity-dependent weight functions and random phases, which in general results into a complex expression.

In the static case, Eq. (1) establishes a direct connection between the two-identical-particle correlation function and the distance  $\Delta r$  as well as the relative direction of the point sources. For moving sources, however, and especially when the velocities are variable, the correspondence is more delicate, as we discuss below.

(a) Let us consider two collinear point sources moving away from each other along the  $x$  axis. For simplicity, let us consider

$$x'^\mu = (t', 0, 0, 0) \text{ and } x''^\mu = (t'', x'', 0, 0), \quad (2)$$

where the second source is accelerated and so with an increasing four-velocity  $u_\mu = (u_0, u_1, 0, 0)$ , each source having a lifetime  $\delta t$ . If we want to measure the longitudinal

distance between the two sources, the most convenient way, according to Eq. (1), is to place the detectors at  $\sim 90^\circ$ , i.e.,  $\mathbf{p} \perp 0x$  (see Fig. 1) and measure  $C(p_1, p_2)$  as a function of  $\Delta \mathbf{p} \parallel 0x (\Delta E = 0)$ . Since  $x''$  is changing, we do not have one distance but many of them. As is well known, if we assume that the spectral distribution is isotropic in the proper frame, in the laboratory frame it becomes concentrated in the forward direction as  $u_1$  increases. Hence, the larger the velocity  $u$  is, the smaller is its contribution to  $\langle \rangle$  of Eq. (1) in the present case. This effect has also been discussed in Ref. 9. The distance  $\Delta x = x''$  that the correlation data reveal would then be the one corresponding to a "typical"  $u$ , obtained with the momentum spectrum as weight function. To be more specific, let us consider, for example, the invariant distribution given by

$$E \frac{dn}{d\mathbf{p}} = u_\mu p^\mu \exp(-u^\mu p_\mu / T) = u_0 E \exp\left[-\frac{u_0 E}{T}\right] \quad (3)$$

for  $\mathbf{p} \equiv \mathbf{p}_T$  ( $p_L = 0$ ). Hence, we have

$$\langle u_0 \rangle = \langle \cosh \alpha \rangle = \frac{K_0(E/T) + K_2(E/T)}{2K_1(E/T)} \stackrel{E \gg T}{\approx} 1 + \frac{1}{2} \frac{T}{E}, \quad (4)$$

where  $K_n(E/T)$  is the modified Bessel function. We see from Eq. (4) that  $\langle u_0 \rangle$  decreases for increasing  $p_T$

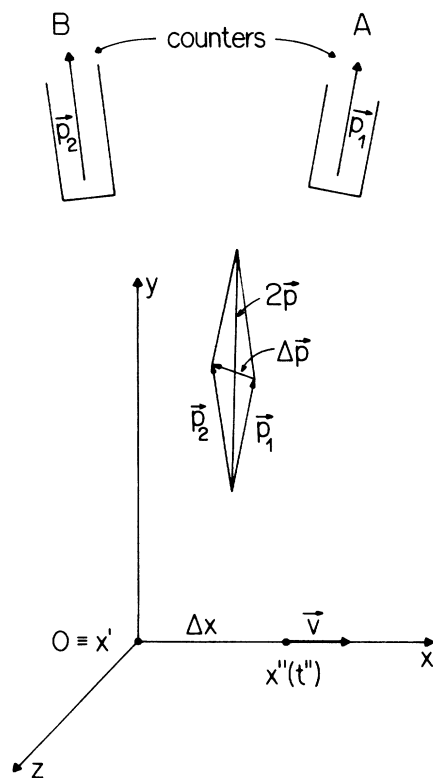


FIG. 1. A schematic representation of relatively moving two point sources. A graphical definition of the vectors  $\mathbf{p}$  and  $\Delta \mathbf{p}$  are also shown.

(i.e.,  $E_T$ ) and that  $u_0 \rightarrow 1$  as  $(T/E) \rightarrow 0$ . To see how this affects the longitudinal distance between the two sources, we assume that  $v = x/t$ , which gives  $\Delta x = x'' = \tau \sinh \alpha$ , where  $\tau = \sqrt{t''^2 - x''^2}$  is the proper time and  $\alpha$  is the rapidity of the second source. Then, for fixed  $\tau$ ,

$$\langle \Delta x \rangle = \tau \langle \sinh \alpha \rangle = \tau \frac{(T/E)(1+T/E)e^{-E/T}}{K_1(E/T)} \approx \left[ \frac{2T}{\pi E} \right]^{1/2} \tau. \quad (5)$$

Equation (5) shows that  $\langle \Delta x \rangle \rightarrow 0$  as  $(T/E) \rightarrow 0$ . This implies that the effective longitudinal size shown by the correlation data decreases as  $p_T$  (or  $E$ ) increases, an effect already shown in Ref. 8 and also discussed in Ref. 11.

(b) Let us now consider the measurement of the transverse "distances" between the source points. For the configuration given by Eq. (2) it is evident that such "distances" are identically zero, but in general  $x''^\mu$  may have  $y''$  and  $z''$  components. To determine  $\Delta z$ , it is natural to put the detectors nearly parallel to the  $y$  axis ( $\mathbf{p} \parallel 0y$ ) and measure  $C(p_1, p_2)$  as a function of  $\Delta p_z$  ( $\Delta E = 0$ ). To estimate  $\Delta y$ , one simply turns the counters by  $\pi/2$  and repeats the procedure. One might think that it is possible to evaluate  $\Delta y$  by setting the detectors along the  $y$  axis and measuring  $C(p_1, p_2)$  as a function of  $\Delta p_y$  (in the case of extended source, it would be equivalent to probing the source's depth). For nonsimultaneous emissions, i.e.,  $\Delta t = t'' - t' \neq 0$ , the argument of the cosine in Eq. (1) becomes

$$\begin{aligned} \Delta p^\mu \Delta x_\mu &= \Delta E \Delta t - \Delta p_y \Delta y \\ &= \Delta p_y \left[ \frac{\Delta E}{\Delta p_y} \Delta t - \Delta y \right] \xrightarrow{\Delta y = 0} \Delta p_y \left[ \frac{\Delta E}{\Delta p_y} \Delta t \right]. \end{aligned} \quad (6)$$

So, although the actual  $\Delta y$  is zero for the two point sources of Eq. (2), it appears as if  $\Delta y = -(\Delta E / \Delta p_y) \Delta t \approx -v \Delta t$ . This effect evidently is a consequence of different emission times, as has already been discussed a long time ago by Kopilov and Podgoretsky<sup>12</sup> (see also Ref. 13), and such a delay is a basic feature of any more realistic model of expanding objects. More generally, when dealing with extended sources, usually  $\Delta y \neq 0$  and is variable. Furthermore, the experimentally measured "depth" would have to be averaged over events, resulting in

$$\begin{aligned} (\Delta y_{\text{eff}})^2 &\simeq \left\langle \left[ \frac{\Delta E}{\Delta p_y} \Delta t - \Delta y \right]^2 \right\rangle \\ &\simeq \left\langle \left[ \frac{\Delta E}{\Delta p_y} \Delta t \right]^2 \right\rangle + \langle (\Delta y)^2 \rangle. \end{aligned} \quad (7)$$

If we consider the asymptotic one-dimensional hydrodynamical model, as in the following sections, and choose to analyze, for example, the correlation of two quanta, one emitted by a central fluid element and the other by an element with rapidity  $\alpha$ , then for fixed  $\tau$ ,  $\Delta t = \tau(\cosh \alpha - 1) > 0$ . Hence, according to the discussion that followed Eq. (4) and to Eq. (7), the transversal depth for

small  $p_T$  will be bigger than the actual one.

(c) So far, we have restricted ourselves to the study of the correlation as a function of one component of  $\Delta\mathbf{p}$ , taking the other components equal to 0. Clearly, such configurations are highly improbable. This is a very important point when one tries to extract information on the source structure from the data, because if, say, the component of  $\Delta\mathbf{p}$  which is parallel to  $\mathbf{p}$  is  $\neq 0$  and the correlation is seen as a function of a normal component of  $\Delta\mathbf{p}$ , for instance  $\Delta p_x$ , first it will not be  $=2$  at the origin ( $\Delta p_x=0$ ) but  $<2$  and also  $\Delta p_x=0$  will not be the point of maximum of  $C(p_1, p_2)$ . Obviously, this implies that a simple parametrization of the data by Eq. (1) or by a Bessel function as usually done in the case of a continuous source may lead to completely erroneous conclusions. To show these effects, let us again consider the two-point source of Eq. (2) and now set the detectors so as to have  $\mathbf{p} \parallel 0y$  and  $\Delta\mathbf{p}=(\Delta p_x, \Delta p_y, 0)$ , with  $\Delta p_y > 0$  constant. Then,  $\Delta p^\mu \Delta x_\mu = \Delta E \Delta t - \Delta p_x \Delta x$ , which gives  $\Delta p^\mu \Delta x_\mu > 0$  when  $\Delta x = 0$  and  $C(p_1, p_2) < 2$  there. The maximum of  $C(p_1, p_2)$  is located at  $\Delta p_x = \Delta E \Delta t / \Delta x > 0$ .

### III. HYDRODYNAMICAL MODEL

Let us now extend the discussion given in the preceding section to a more realistic extended source that we will describe by a variant of the Landau model<sup>14</sup> in which we assume that the fluid is the quark-gluon plasma<sup>8,11</sup> and the fireball mass is an event-dependent parameter. While the latter assumption is not necessary if we confine ourselves just to a theoretical study of the expansion effect on the correlation, it turns out to be essential when comparing the results with the existing data.<sup>15</sup>

Since the final results are not expected to be very sensitive to the details of the expansion model, here we completely neglect the transverse expansion and use the asymptotic form of the Khalatnikov solution:<sup>16</sup> namely,

$$\xi \equiv \ln \frac{T}{T_0} \simeq -c_0^2 \ln \frac{\tau}{\Delta}, \quad (8)$$

$$\alpha \simeq \frac{1}{2} \ln \frac{t+x}{t-x}, \quad (9)$$

where  $\alpha$  is the rapidity of the plasma,  $c_0$  the sound velocity  $\simeq 1/\sqrt{3}$  and  $\Delta = \sqrt{(1-c_0^2)/\pi} l$ ,  $2l$  is the initial thickness of the fireball. This solution is valid when  $|\xi| \gg |\alpha|$ .

Usually, one assumes that the final particles appear when the local temperature reaches a certain critical value  $T = T_c \simeq m_\pi$ , which defines a transition surface. However, because of the statistic factor, which is large in the quark-gluon plasma, its energy density  $\epsilon_p(T_c)$  is too high to assume that pions appear from such a surface. We think it is more reasonable to let the fluid expand further and assume that the final-particle emission occurs during this interval of time when the energy density goes down to the characteristic value for the hadronic gas  $\epsilon_h(T_c)$ . Since the pressure remains constant during the transition, the expansion in this stage is expected to be inertial,  $\alpha$  in Eq. (9) being unchanged. Here, we shall first study the problem under the assumption that particles

are emitted at  $\tau = \tau_c$ , when  $\epsilon = \epsilon_p(T_c)$  and then improve the results in the next section, by considering the above effect, but for simplicity taking  $\tau = \langle \tau \rangle \propto \tau_c$ , where  $\langle \tau \rangle$  is a certain average value which will be computed later. Evaporation from the hot plasma would certainly exist but here we assume that the bulk of the produced particles comes from the transition region which develops from inside to outside. The effects of resonance production, final-state interactions,<sup>3</sup> as well as of the partial coherence of the source,<sup>3,7</sup> if any, should be taken into account, but here we simply consider a totally chaotic source, which will be shown (Sec. IV) to be surprisingly well fitted to reproduce the existent data.

So, let us initially assume that each point of the surface  $\tau = \tau_c$  in the plasma where  $T = T_c \simeq m_\pi$  is an independent chaotic source with the momentum spectrum

$$f(p) \simeq \frac{1}{(2\pi)^3} \frac{u^\mu p_\mu}{E} \exp\left[-\frac{u^\mu p_\mu}{T_c}\right], \quad (10)$$

where

$$\begin{aligned} u^\mu &= (\cosh\alpha, \sinh\alpha, 0, 0) \\ &= \text{four-velocity of the fluid,} \\ p^\mu &= (E, p_x, p_y, p_z) \\ &= \text{four-momentum of an emitted particle.} \end{aligned} \quad (11)$$

The amplitude for finding a particle at  $x$  and emitted at  $x'$  is written

$$J(x, x') = \int d\mathbf{p} \sqrt{f(p)} \exp[-ip_\mu(x^\mu - x'^\mu)] \exp[i\theta(x')], \quad (12)$$

where  $\theta(x')$  is a random phase. Following the notation of Ref. 5, the probability of detecting two quanta of momenta  $p_1$  and  $p_2$  in an event is

$$W(p_1, p_2) = \bar{I}(0, p_1) \bar{I}(0, p_2) + |\bar{I}[p_1 - p_2, \frac{1}{2}(p_1 + p_2)]|^2, \quad (13)$$

where

$$\begin{aligned} \bar{I}(\Delta p, p) &= \int dx d\Delta x \exp(ix\Delta p + i\Delta xp) \\ &\quad \times \int dx' I(x, \Delta x, x'), \\ \left\langle J^* \left[ x - \frac{\Delta x}{2}, x' \right] J \left[ x + \frac{\Delta x}{2}, x'' \right] \right\rangle &= \delta(x' - x'') \\ &\quad \times I(x, \Delta x, x'), \end{aligned} \quad (14)$$

and the average is taken over the random phases  $\theta(x')$  and  $\theta(x'')$ . We also have

$$\begin{aligned} W(p_i) &\equiv \left\langle \left| \int dx' \int \exp(ip_i x) J(x, x') dx \right|^2 \right\rangle \\ &= \bar{I}(0, p_i). \end{aligned} \quad (15)$$

Thus, by inserting Eqs. (10)–(12) into (14) and then  $\bar{I}(\Delta p, p)$  so obtained into Eqs. (13) and (15), we can easily calculate the correlation coefficient  $C(p_1, p_2)$  defined by Eq. (1), giving

$$\begin{aligned}
C(p_1, p_2) = & 1 + \frac{4[J_i(R\Delta p_T)]^2}{T_c R^2 \Delta p_T^2} \left[ \exp \left[ -2 \left\{ \left[ \left( \frac{E^2 - p_L^2}{2T_c^2} - \frac{\Delta E^2 - \Delta p_L^2}{2} \tau_c^2 \right)^2 + (E\Delta E - p_L \Delta p_L)^2 \frac{\tau_c^2}{T_c^2} \right]^{1/2} \right. \right. \right. \\
& \left. \left. \left. + \frac{E^2 - p_L^2}{2T_c^2} - \frac{\Delta E^2 - \Delta p_L^2}{2} \tau_c^2 \right\}^{1/2} \right] \right] / \left[ \left[ \frac{E^2 - p_L^2}{T_c^2} - (\Delta E^2 - \Delta p_L^2) \tau_c^2 \right] \right. \\
& \left. \left. + 4(E\Delta E - p_L \Delta p_L)^2 \frac{\tau_c^2}{T_c^2} \right]^{3/4} \right. \\
& \times \left[ \exp \left\{ \frac{1}{T_c} \left[ \left[ E^2 - p_L^2 + \frac{\Delta E^2 - \Delta p_L^2}{4} + (E\Delta E - p_L \Delta p_L) \right]^{1/2} \right. \right. \right. \\
& \left. \left. \left. + \left[ E^2 - p_L^2 + \frac{\Delta E^2 - \Delta p_L^2}{4} - (E\Delta E - p_L \Delta p_L) \right]^{1/2} \right] \right\} \right] / \left[ \left[ E^2 - p_L^2 + \frac{\Delta E^2 - \Delta p_L^2}{4} \right]^2 \right. \\
& \left. \left. - (E\Delta E - p_L \Delta p_L)^2 \right]^{1/4} \right. \\
& \times \left[ \left[ \left[ \frac{E^2 - p_L^2}{T_c} \right]^2 + \left[ \frac{E\Delta E - p_L \Delta p_L}{2T_c} \right]^2 + (E\Delta E - p_L \Delta p_L)^2 \tau_c^2 + \frac{(\Delta E^2 - \Delta p_L^2)^2}{4} \tau_c^2 \right] \right. \\
& \left. \left. - \left[ \frac{E^2 - p_L^2}{T_c} + (\Delta E^2 - \Delta p_L^2) \tau_c^2 \right] (E\Delta E - p_L \Delta p_L)^2 \right]^{1/2} \right. , \tag{16}
\end{aligned}$$

where

$$\begin{aligned}
p & \equiv \frac{1}{2}(p_1 + p_2) = (E, p_L, p_y, p_z) , \\
\Delta p & \equiv p_1 - p_2 = (\Delta E, \Delta p_L, \Delta p_y, \Delta p_z) , \\
\Delta p_T & = (\Delta p_y^2 + \Delta p_z^2)^{1/2} .
\end{aligned} \tag{17}$$

We fix the critical temperature  $T_c = m_\pi$  and  $\tau_c$  shall be determined by imposing the condition  $T = T_c$  on the plasma. To do so, we need the initial temperature  $T_0$ , which depends on the mass  $M$  of the fireball and its initial size. It has been shown that the hypothesis of large-mass Lorentz-contracted fireball formation around one or both of the incident particles provides a nice framework to account for several of the experimentally observed quantities.<sup>17,18</sup> In Ref. 18 it has been shown that, if such a fireball is made of quarks and gluons, a very reasonable choice of the initial radius  $R \simeq R_{\text{proton}}$  leads to the experimentally observed mean charged multiplicity  $\langle N_{\text{ch}} \rangle(M)$  as well as to the pseudorapidity distribution  $d\sigma/d\eta(M)$ , which have recently been measured in large-mass

diffractive dissociation at the  $\bar{p}p$  collider.<sup>19</sup> In contrast, if such a fireball is made of pions, a too large radius  $R$  becomes necessary to fitting the data. It would also be possible to impose some other initial conditions wherein non-constant space-time distributions of temperature and velocity are specified,<sup>20,21</sup> but in this case we would not have a definite principle for such an assignment and, moreover, a simple version in which  $T$  and  $v$  are specified on a hyperbola  $\tau = \text{const}$  gives exactly the same asymptotic Khalatnikov's solution. As far as the practical results are concerned, we can go backward in time and start from a constant temperature  $T = T_0$  and  $v = 0$  at  $t = 0$ . Then, following Ref. 18,

$$\begin{aligned}
T_0 & = \left[ \frac{45}{4\pi^3 m_p R^3 (g_g + \frac{7}{8}g_q)} \right]^{1/4} \sqrt{M} = b\sqrt{M} \\
& \simeq 0.118\sqrt{M} ,
\end{aligned} \tag{18}$$

where  $g_g$  and  $g_q$  are the statistical weights of gluons and quarks, respectively, and the numerical value of  $b$  in the last equality has been fixed (in  $\text{GeV}^{1/2}$ ), by using the fit

$\langle N_{\text{ch}} \rangle \approx 1.8\sqrt{M}$  (which means  $R=0.76$  fm if  $N_f=2$  as is taken throughout this section). Then, from Eq. (8) we have

$$\tau_c^2 = \Delta^2 \left( \frac{T_0}{T_c} \right)^6 = \frac{8m_p^2}{3\pi} \left( \frac{b}{m_\pi} \right)^6 (R^2 M) \approx 3.88M. \quad (19)$$

We shall now illustrate the kinematical effects discussed in Sec. II, by using Eq. (16) above. Let us first consider two equal energy quanta emitted symmetrically with respect to some transverse direction and plot  $C(p_1, p_2)$  as a function of  $\Delta p = |\mathbf{p}_2 - \mathbf{p}_1|$ . We show in Fig. 2, curves with  $\Delta p_L = 0$  and  $\Delta p_T = 0$  at two different values of  $M$ . In the  $\Delta p_L = 0$  case ( $\Delta p = \Delta p_T$ ), the correlation coefficient does not show any  $M$  dependence because the transverse dimensions remain constant in the present version and independent of the energy. On the other hand, in the  $\Delta p_T = 0$  case ( $\Delta p = \Delta p_L$ ), a strong  $M$  dependence of  $C(p_1, p_2)$  does appear. This effect can easily be understood if we notice that according to Eqs. (8) and (9) the surface  $T = T_c$  from which the hadrons emerge is a hyperbola which moves upward as the mass  $M$  increases (see Fig. 3) and curves with constant velocities are straight lines starting from the origin of the coordinate frame 0, namely,  $x = vt$ , which means as discussed before that the correlation in  $\Delta p_L$  decreases (apparent size increases) with  $M$ .

Let us now study the  $p_T$  dependence of the correlation. We show in Fig. 4 two families of curves corresponding to two different arrangements of counters, each curve

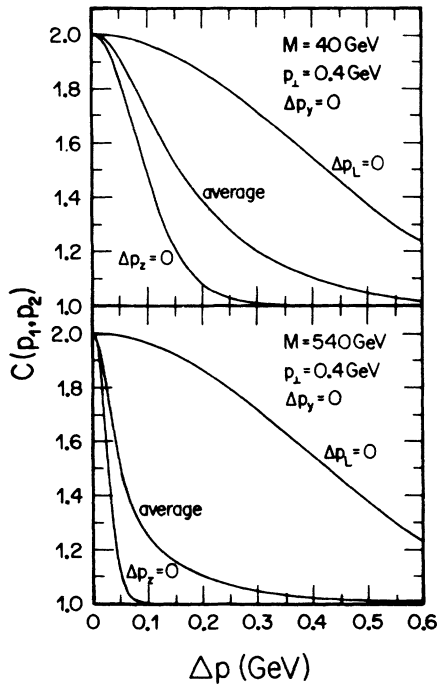


FIG. 2. Correlation parameter given by Eq. (16), as a function of  $\Delta p = |\mathbf{p}_1 - \mathbf{p}_2|$ , when  $\mathbf{p}_1$  and  $\mathbf{p}_2$  are symmetrical with respect to some transverse direction. The coordinate axes have been chosen as in Fig. 1, with 0x parallel to the expansion direction,  $\Delta p_L \equiv \Delta p_x$ . The curves labeled *average* correspond to the mean values taken over the azimuthal angle with respect to  $\mathbf{p}$ .

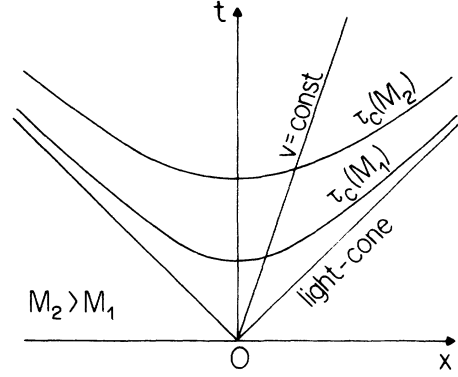


FIG. 3. Graphical representation of the transition surface  $T = T_c$  (or  $\tau = \tau_c$ ) for two different values of the fireball mass  $M$ . The straight line indicates the curve  $v = \text{const}$ .

computed with a fixed average transverse momentum  $p_T$  of the two quanta. Their average direction has been set to be  $\pi/2$  with respect to the longitudinal axis and the curves in Fig. 4(a) represent the longitudinal-momentum correlation whereas those in Fig. 4(b) correspond to the one with  $\Delta \mathbf{p} \parallel \mathbf{p}$  (source-depth measurement). In both the cases, one clearly sees that as  $p_T$  increases the width of  $C(p_1, p_2)$  increases as well, mimicking a diminution of

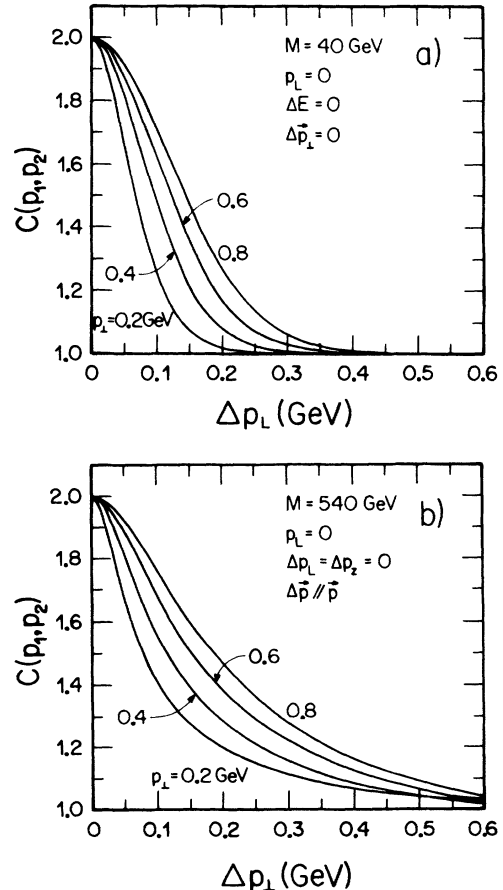


FIG. 4.  $p_T$  dependence of the correlation coefficient (a) as a function of  $\Delta p_L$  at  $M=40$  GeV and (b) as a function of  $\Delta p_T$  at  $M=540$  GeV.

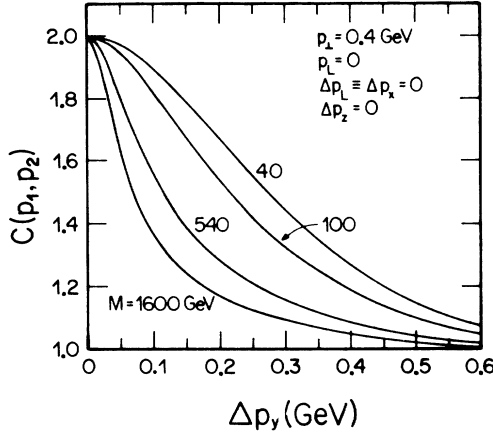


FIG. 5. Fireball mass dependence of the correlation coefficient as a function of  $\Delta p_y$ .

the effective source size, in agreement with our previous discussion in Sec. II.

It is also interesting to see the fireball-mass dependence of the correlation coefficient as a function of  $\Delta p_y$ , as displayed in Fig. 5 (the axes have been chosen as in Fig. 1, where the fireball expands along the  $x$  axis). For all these curves the transverse dimensions of the source are the same, difference occurring only in the longitudinal expansion. As discussed in Sec. II [Eqs. (3) and (4) and below], once the average energy of the identical particles is fixed, the average velocity of the effective source  $\langle u \rangle$  is also defined. Now, by looking at Fig. 3 one notes that for the same velocity of the fluid the time  $\Delta t$  becomes larger as  $M$  increases, yielding due to Eq. (6) larger apparent depth for the source or narrower curve for  $C(p_1, p_2)$ .

Let us now examine some more probable cases of  $\Delta p$  dependence of the correlation, in which more than one component of  $\Delta p$  are  $\neq 0$ . Figure 6 displays some examples where the correlation has been computed at an average direction of  $\pi/2$  with respect to the symmetry axis and with  $\Delta p_y \neq 0$ . In each case,  $C(p_1, p_2)$  is plotted as a function of  $\Delta p'$ , where  $\Delta p' = (\Delta p_x^2 + \Delta p_z^2)^{1/2}$ . The main

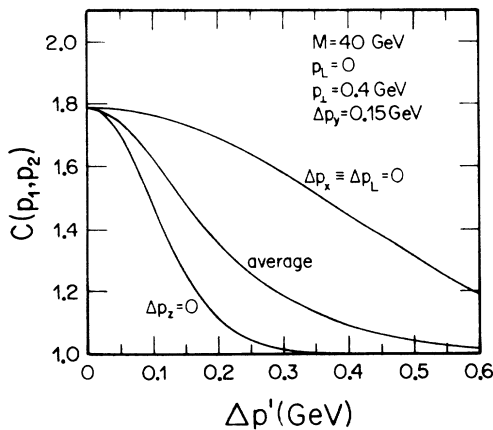


FIG. 6. Correlation coefficient with  $\Delta p_y \neq 0$ , as a function of  $p' = (\Delta p_x^2 + \Delta p_z^2)^{1/2}$ .

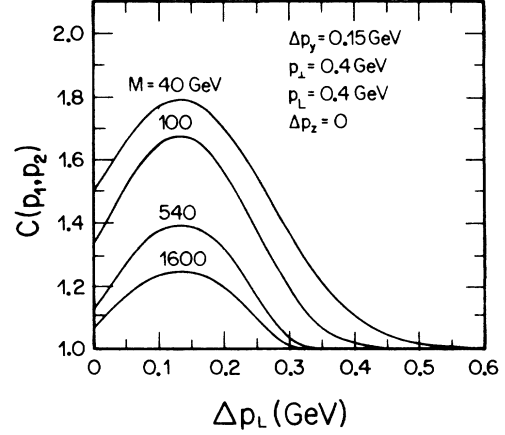


FIG. 7. Correlation coefficient with  $\Delta p_y \neq 0$  and  $p_L \equiv p_x \neq 0$ , as a function of  $\Delta p_L \equiv \Delta p_x$ .

feature of these curves is the fact that  $C(p_1, p_2) < 2$  at the origin  $\Delta p' = 0$ , which is quite natural since here  $\Delta p' = 0$  does not imply  $\Delta p = 0$ . As we have already discussed in the previous section (and here we emphasize it again) data are never obtained with, say,  $\Delta p_y = 0$ , but within a certain limit, so the experimentally measured correlation coefficient is always smaller than 2, even if the source is totally chaotic. Also, the maximum of  $C(p_1, p_2)$  is not necessarily at  $\Delta p' = 0$ . Although this is the case for the curves in Fig. 6, this feature can more clearly be seen when one looks at Fig. 7, where we show  $C(p_1, p_2)$  as a function of  $\Delta p_x$  when  $\Delta p_y \neq 0$  and the average direction of the two quanta are not at right angles with respect to the expansion axis ( $p_L \neq 0$ ).

#### IV. COMPARISON WITH DATA

In the previous section, we have shown several kinematical effects that the source expansion causes on the correlation by considering a hydrodynamical model where the source is a quark-gluon plasma which is assumed to be formed during a hadronic collision and which emits the observed pions as it cools by expansion and reaches the critical temperature  $T_c \simeq m_\pi$ . As has been mentioned there, due to the large statistical factor in the quark-gluon plasma, its critical energy density  $\epsilon_p(T_c)$  is much higher than the characteristic hadronic energy density  $\epsilon_h(T_c)$ . Then, in order to compare the results with the data,<sup>15</sup> a more realistic model is needed, whereby the fluid expands further undergoing a phase transition. Particle emission occurs during this time interval in which the energy density decreases from  $\epsilon_p(T_c)$  down to  $\epsilon_h(T_c)$ .

In estimating the correlation coefficient with the phase transition taken into account, we assume following Gyulassy and Matsui<sup>22</sup> that an isentropic path is followed during such a transition. Then, because our fluid is one dimensional (with the transverse expansion neglected) and is expected to undergo an inertial expansion during this stage as argued in Sec. III, the fluid velocity remains  $v = x/t = \text{const}$  and

$$s\tau = s_p\tau_p = s_h\tau_h \quad (\tau_p \leq \tau \leq \tau_h), \quad (20)$$

where  $s_p$  and  $\tau_p$  are, respectively, the entropy density and the (proper) time when the transition begins and  $s_h$  and  $\tau_h$  are the same quantities at the end of the transition. We assume the entropy density  $s_p$  as being the one of a (massless) noninteracting quark-gluon plasma

$$s_p = g_p \frac{2\pi^2}{45} T_c^3, \quad (21)$$

with the effective number of freedom  $g_p = 2 \times 8 + 7 \times (2 \times 3 \times 2 \times N_f)/8$ ,  $N_f$  being the number of quark flavors, and  $s_h$  that of the usual pion + kaon ideal gas, namely,

$$s_h = \frac{1}{2\pi^2} [g_\pi G(z_\pi) + g_K G(z_K)] T_c^3, \quad (22)$$

where  $g_\pi = 3$ ,  $g_K = 4$ ,  $z_i = m_i/T_c$ , and

$$G(z) = z^2 \sum_{n=1}^{\infty} \frac{4K_2(nz) + nzK_1(nz)}{n^2}. \quad (23)$$

So, with the use of Eqs. (18) and (19) (the numerical value of  $b$  now has to be changed to 0.099 because our hadronic gas contains kaons as well as pions), we get

$$\tau_h = \frac{s_p}{s_h} \tau_c = \frac{(4\pi^4/45)g_p}{g_\pi G(z_\pi) + g_K G(z_K)} \tau_c, \quad (24)$$

where  $G(z_\pi \simeq 1) \simeq 7.476$ ,  $G(z_K \simeq 3.5) \simeq 2.156$ , and  $\tau_c$  is given by Eq. (19).

At a given instant of time in the interval  $\tau_p \leq \tau \leq \tau_h$ , we have

$$s = fs_p + (1-f)s_h, \quad 0 \leq f \leq 1; \quad (25)$$

i.e., the total entropy density of the fluid is a sum of a plasma portion and a hadronic portion, so that  $s = s_p$  at  $\tau = \tau_p$  and  $s = s_h$  at  $\tau = \tau_h$ . It immediately follows that

$$f = \frac{\tau_h - \tau}{\tau_h - \tau_p} \frac{\tau_p}{\tau}, \quad (26)$$

which is the fraction of the mixture that is still in the plasma phase. We think this portion of the entropy, namely,

$$s_f \equiv fs_p = \frac{\tau_h - \tau}{\tau_h - \tau_p} \frac{\tau_p s_p}{\tau} \quad (27)$$

(in terms of density) should properly be considered as the particle-emission source during the transition.

So, a more exact calculation of  $C(p_1, p_2)$  would amount to including the factor given in Eq. (27) into Eq. (12) or (14) of the previous section, where the integration has been simplified by  $\delta(\tau - \tau_c)$  assumed there. However,

as will be discussed below, this is not the whole story. In order to get quantities comparable with the data,<sup>15</sup> more integrations or averaging processes are required. In the present paper we instead preferred to simplify the problem and estimate  $C(p_1, p_2)$  by considering “typical” values of all these integration variables and computing it there. Thus, instead of performing a detailed  $\tau$  integration in Eq. (14) (see details in Ref. 8) with an additional factor  $f$  given by Eq. (26), we have computed the average time

$$\langle \tau \rangle = \frac{\frac{1}{2} \left[ \frac{\tau_h}{\tau_c} - 1 \right]^2}{\frac{\tau_h}{\tau_c} \left[ \ln \frac{\tau_h}{\tau_c} - 1 \right] + 1} \tau_c \quad (28)$$

with  $s_f$  taken as the weight function and then replaced  $\tau_c$  by  $\langle \tau \rangle$  in Eq. (16). In Table I, we show the numerical estimates for  $\tau_h/\tau_c$  and  $\langle \tau \rangle/\tau_c$  when  $N_f = 2$  or 3 and the hadron gas is made of pions and kaons.

Now, as stressed at the end of Sec. III, we should not forget that the kinematical situations chosen there are highly ideal. Because of the low statistics, the available correlation data have been obtained by considering pairs of identical particles in much wider kinematical domains. For instance, in Ref. 15, data were obtained for  $pp$  collisions at  $\sqrt{s} = 53$  GeV, by detecting all  $\pi^+$  mesons with  $p_T \geq 0.1$  GeV and in the rapidity range of  $|y| \lesssim 1.0$ . Then, the correlation of such pions is determined by taking all the pairs into account and as a function of  $q_L$ , with  $q_T \lesssim 0.15$  GeV or as a function of  $q_T$ , with  $q_L \lesssim 0.15$  GeV. Here,  $q_L$  (and  $q_T$ ) are the usual Kopilov's variables,<sup>4</sup> namely, the components of  $\Delta \mathbf{p}$  which are parallel (and orthogonal) to  $\mathbf{p} = (\mathbf{p}_1 + \mathbf{p}_2)/2$ .

Thus, in order to make comparisons with experimental data, we should average our result given by Eq. (16) over several of the kinematical variables. However, inclusion of all this averaging procedures makes the computation much more complex, so for the sake of simplicity we decided to invert it and estimate  $C(p_1, p_2)$  by adopting some “typical” (i.e., average) values of all the variables but one, namely,  $q_T$  or  $q_L$ , as function of which the data are given. The only averaging which has explicitly been carried out is the one over the azimuthal angle with respect to the “typical” momentum  $\mathbf{p}$  taken from data.

We present the results of this evaluation in Figs. 8 and 9, together with the data of Ref. 15. As can be seen the agreement is quite good and especially in Fig. 8(a) one sees that, although our source is *completely chaotic*,  $q_T$  dependence of  $\langle C(p_1, p_2) \rangle$  for  $\pi^+ \pi^+$  is much better reproduced by our curves than by the empirical fit

TABLE I. Numerical estimates of  $R$ ,  $\tau_c$  (at  $M = 40$  GeV),  $\tau_h/\tau_c$ , and  $\langle \tau \rangle/\tau_c$ , under the assumption of pion + kaon gas at the final state.

$N_f$	$R$ (fm)	$\tau_h/\tau_c$	$\langle \tau \rangle/\tau_c$	$\tau_c$ (at $M = 40$ GeV) (fm)
2	0.95	10.32	2.94	1.83
3	0.88	13.24	3.41	1.70

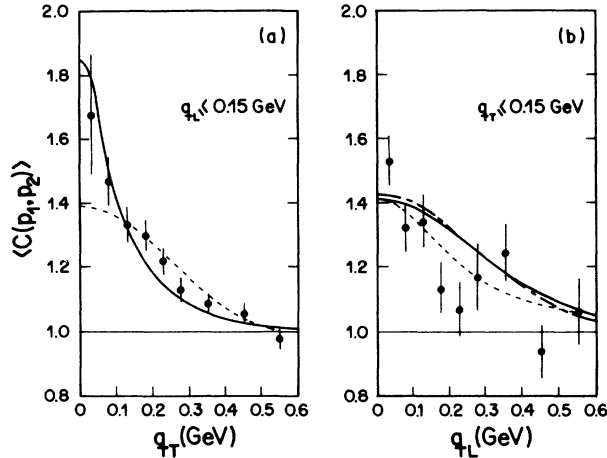


FIG. 8. Average  $\pi^+\pi^+$  correlation coefficient, computed as explained in the text, is compared with the experimental data (Ref. 15). The solid curves are our estimates with  $N_f=3$  ( $g_p=47.5$ ), the dotted-dashed lines with  $N_f=2$  ( $g_p=37$ ), whereas the dashed lines are the empirical fits given in Ref. 15. In accordance with the experimental conditions, we have taken  $\langle M \rangle = 37.5$  GeV,  $\langle p_T \rangle = 0.38$  GeV,  $\langle \theta \rangle = 1.01$  rad, and in (a)  $\langle q_L \rangle = 0.075$  GeV and in (b)  $\langle q_L \rangle = 0.1$  GeV.

presented there. Observe that we have not adjusted any parameter by fitting the data, but all the numerical parameters have been predetermined either by the experimental conditions described in Ref. 15 or by theoretical considerations (as  $T_c \simeq m_\pi$  and  $g_p$ ). It is interesting to notice that no appreciable difference in  $\langle C(p_1, p_2) \rangle$  is introduced by changing the number of quark flavors. This is, in our opinion, due mostly to the fact that the data are the average over several pion-momentum directions, so that mainly those pairs which are relatively insensitive to the collective motions give contributions to the data. We think that in analyzing data if one enhances the longitudinal ( $\Delta p_L$ ) correlation, one can better discriminate among several possibilities.

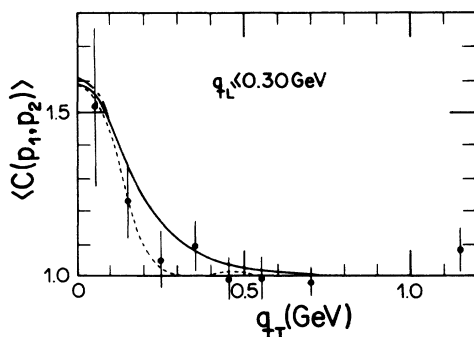


FIG. 9. Average  $KK$  correlation coefficient, computed as explained in the text, is compared with the experimental data (Ref. 15). The symbols are the same as those employed in Fig. 8. Following the experimental conditions, we have taken  $\langle M \rangle = 40$  GeV,  $\langle p_T \rangle = 0.44$  GeV,  $\langle \theta \rangle = 0.85$ , and  $\langle q_L \rangle = 0.15$  GeV.

## V. CONCLUSIONS

We have studied in the present paper several kinematical effects which a rapid expansion of the source may cause on the correlation between two identical particles emitted in a high-energy hadronic collision. This has been schematized by a simple two-point-source model in Sec. II and then extended to a continuous chaotic source in Sec. III, by using the scaling solution of the hydrodynamical equations as such a source.

We have shown that, for expanding sources, what one actually measures in correlation experiments are the source dimensions characterized by some typical collective four-velocity  $u_0 \leq \langle u_0 \rangle$ , which is  $p_T$  dependent, as in Eq. (4). In particular, as estimated in Eq. (5) and exhibited in Fig. 4(a), the longitudinal dimension decreases as  $p_T$  increases.

The  $q_L$  dependence of the correlation coefficient does not directly show the source depth but a combined effect of the depth and the emission time interval, both in the velocity range mentioned above. Furthermore, the effective transversal depth for small  $p_T$  is bigger than the actual one, due to the difference in emission times, and also decreases for increasing  $p_T$ , as shown in Fig. 4(b).

Experimentally, all the components of  $\mathbf{p}$  are generally nonzero. Thus, e.g.,  $q_T \neq 0$  if one is plotting  $C(p_1, p_2)$  as a function of  $q_L$ . It follows that *the experimental  $C(p_1, p_2)$  is always smaller than 2 at the origin ( $q_L = 0$ ) without implying necessarily that the source be coherent.* In this paper, we have taken a completely chaotic source which has shown to be enough to reproducing the data.

The correlation is shown to be strongly dependent on the mass  $M$  of the fireball. By varying the incident energy  $\sqrt{s}$ , one may experimentally study its average mass ( $\langle M \rangle$ ) dependence. In Figs. 10 and 11 we show some predictions for such an energy dependence of  $\pi^+\pi^+$  (or  $\pi^-\pi^-$ ) correlation at the  $\bar{p}p$  collider energies, by assuming exactly the same kinematical restrictions imposed in Ref. 15. As is seen, the correlation curve becomes narrower as  $s$  increases and also the peak “shrinks” as a consequence of this effect combined with the fact that

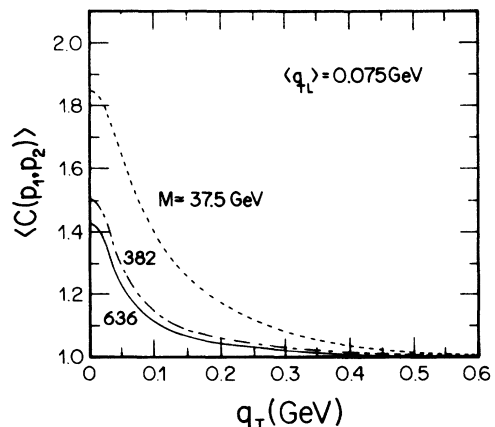


FIG. 10. Energy dependence of the average  $\pi^+\pi^+$  correlation coefficient as a function of  $q_T$ , computed under the assumption of the same kinematical restrictions as in Ref. 15.



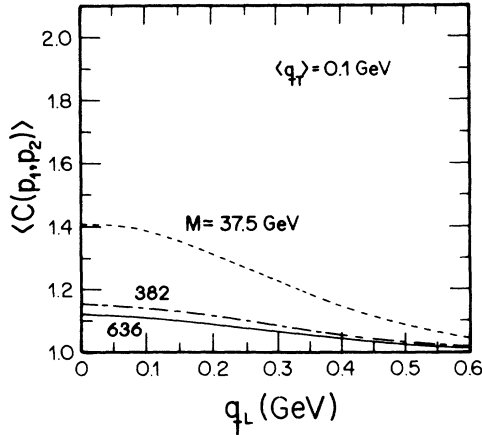


FIG. 11. The same as in Fig. 10, but as a function of  $q_L$ .

$q_L \neq 0$  (Fig. 10) or  $q_T \neq 0$  (Fig. 11). The narrowing is a striking feature to be looked for and is related to the growing of  $\tau_c$  (and hence, of  $\langle \tau_h \rangle$ ) proportionally to  $\sqrt{\langle M \rangle}$  or to  $s^{1/4}$ , according to the asymptotic one-dimensional Landau model. On the other hand, the fireball mass is an event-dependent parameter since, as it is well known, there is a large inelasticity fluctuation in hadronic collisions. Being so, it is also desirable to see how  $\langle C(p_1, p_2) \rangle$  varies with  $M$  at fixed energy  $\sqrt{s}$ .

In comparing with the data, we have assumed forma-

tion of quark-gluon plasma which undergoes a (first-order) transition as it freezes down to a critical temperature. The agreement with data is quite good suggesting that the physical idea behind our model is reasonable.

The averaging over several kinematical variables washes out many of the interesting features of two-particle correlation. This is especially well illustrated by Figs. 2 and 6. Although it may be an arduous task to get statistically reliable data, it is worthwhile to narrow down the kinematical windows, for it will certainly give much richer information on the space-time structure of the hadronic collisions.

In short, we conclude that in high-energy hadronic interferometry, we cannot get any useful information either about the nature of the source or about its dimension without taking the longitudinal expansion effects into account. (After completion of this work we became aware of similar work by Makhlin and Sinyukov.<sup>23</sup>)

#### ACKNOWLEDGMENTS

One of us (S.S.P.) acknowledges the financial support of the Fundação do Amparo à Pesquisa do Estado de São Paulo (FAPESP) and the Coordenadoria de Aperfeiçoamento do Pessoal de Nível Superior (CAPES), Brazil, during the present work. We thank M. Gyulassy for useful comments on this work.

- <sup>1</sup>R. Hanbury-Brown and R. Q. Twiss, *Philos. Mag.* **45**, 663 (1954); *Nature (London)* **178**, 1046 (1956).  
<sup>2</sup>G. Goldhaber, S. Goldhaber, W. Lee, and A. Pais, *Phys. Rev.* **120**, 300 (1960).  
<sup>3</sup>M. Gyulassy, S. K. Kauffmann, and L. W. Wilson, *Phys. Rev. C* **20**, 2267 (1979).  
<sup>4</sup>G. I. Kopilov and M. I. Podgoretsky, *Yad. Fiz.* **14**, 1081 (1971) [*Sov. J. Nucl. Phys.* **14**, 604 (1972)]; **15**, 392 (1972) [**15**, 219 (1972)]; **18**, 656 (1973) [**18**, 336 (1974)]; G. I. Kopilov, *Phys. Lett.* **50B**, 472 (1974); M. I. Podgoretsky, *Yad. Fiz.* **37**, 455 (1983) [*Sov. J. Nucl. Phys.* **37**, 272 (1983)].  
<sup>5</sup>E. V. Shuryak, *Phys. Lett.* **44B**, 387 (1973).  
<sup>6</sup>G. Cocconi, *Phys. Lett.* **49B**, 459 (1974).  
<sup>7</sup>G. N. Fowler and R. M. Weiner, *Phys. Lett.* **70B**, 201 (1977).  
<sup>8</sup>Y. Hama and Sandra S. Padula, in *Hadronic Matter in Collision (LESIP II)*, edited by P. Carruthers and D. Strottman (World Scientific, Singapore, 1986), p. 63.  
<sup>9</sup>B. Andersson and W. Hofmann, *Phys. Lett.* **169B**, 364 (1986).  
<sup>10</sup>K. Kolehmainen and M. Gyulassy, *Phys. Lett. B* **180**, 203 (1986).  
<sup>11</sup>S. Pratt, *Phys. Rev. D* **33**, 1314 (1986).

- <sup>12</sup>G. I. Kopilov and M. I. Podgoretsky, *Yad. Fiz.* **19**, 434 (1974) [*Sov. J. Nucl. Phys.* **19**, 215 (1974)].  
<sup>13</sup>S. Pratt, *Phys. Rev. D* **33**, 72 (1985).  
<sup>14</sup>L. D. Landau, *Izv. Akad. Nauk SSSR Ser. Fiz.* **17**, 51 (1953); *Collected Papers of L. D. Landau*, edited by D. Ter Haar (Pergamon, Oxford, 1965), p. 569.  
<sup>15</sup>Axial-Field-Spectrometer Collaboration, T. Akesson *et al.*, *Phys. Lett.* **129B**, 269 (1983); **155B**, 128 (1985).  
<sup>16</sup>I. M. Khalatnikov, *Zh. Eksp. Teor. Fiz.* **26**, 529 (1954).  
<sup>17</sup>Y. Hama, *Phys. Rev. D* **19**, 2623 (1979); Y. Hama and F. W. Pottag, *Rev. Bras. Fis.* **12**, 247 (1982); Y. Hama and F. S. Navarra, *Phys. Lett.* **129B**, 251 (1983); *Z. Phys. C* **26**, 465 (1984).  
<sup>18</sup>Y. Hama and F. W. Pottag (in preparation).  
<sup>19</sup>UA4 Collaboration, D. Bernard *et al.*, *Phys. Lett.* **166B**, 459 (1986).  
<sup>20</sup>J. D. Bjorken, *Phys. Rev. D* **27**, 140 (1983).  
<sup>21</sup>K. Kajantie and L. McLerran, *Phys. Lett.* **119B**, 203 (1982).  
<sup>22</sup>M. Gyulassy and T. Matsui, *Phys. Rev. D* **29**, 419 (1984).  
<sup>23</sup>A. N. Makhlin and Yu. M. Sinyukov, *Kiev Report No. ITP-87-64E*, 1987 (unpublished).